^{118}Sn levels studied by the ^{120}Sn(p, t) reaction: High-resolution measurements, shell model, and distorted-wave Born approximation calculations

P. Guazzoni and L. Zetta
Dipartimento di Fisica dell'Università and Istituto Nazionale di Fisica Nucleare, Via Celoria 16, I-20133 Milano, Italy

A. Covello and A. Gargano
Dipartimento di Scienze Fisiche, Università di Napoli Federico II, Complesso Universitario di Monte S. Angelo Via Cintia, I-80126 Napoli, Italy and Istituto Nazionale di Fisica Nucleare, Complesso Universitario di Monte S. Angelo Via Cintia, I-80126 Napoli, Italy

B. F. Bayman
School of Physics and Astronomy, University of Minnesota, Minneapolis, Minnesota 55455, USA

T. Faestermann, G. Graw, R. Hertenberger, and H.-F. Wirth
Sektion Physik der Universität München, D-85748 Garching, Germany

M. Jaskola
Soltan Institute for Nuclear Studies, Warsaw, Poland

(Received 17 September 2008; published 15 December 2008)

Cross-section angular distributions of 38 (p, t) transitions to final states of ^{118}Sn up to an excitation energy of 3.597 MeV have been measured in a high-resolution experiment at an incident proton energy of 21 MeV. A distorted-wave Born approximation (DWBA) analysis of the 38 experimental differential cross sections, carried out by using conventional Woods-Saxon potentials, allowed us either 18 confirmations of previous spin and parity values or new assignments of spin and parity to 14 states of ^{118}Sn. A shell-model calculation has been performed by using a realistic two-body effective interaction derived from the CD-Bonn nucleon-nucleon potential. The doubly-magic nucleus ^{132}Sn is assumed as a closed core, with 14 valence neutron holes occupying the five levels of the 50–82 shell. Within this model space the calculations are performed by employing the seniority scheme including states with seniority up to 4. The energy spectrum of ^{118}Sn has been calculated and compared with the experimental one. The theoretical two-neutron spectroscopic amplitudes are used in the microscopic DWBA calculations of some cross-section angular distributions.

DOI: 10.1103/PhysRevC.78.064608 PACS number(s): 25.40.Hs, 21.10.Hw, 21.60.Cs, 27.60.+j

I. INTRODUCTION

The tin isotopes, with 10 stable isotopes from ^{112}Sn to ^{124}Sn, provide a very good opportunity for experimental and theoretical investigations of the variation of nuclear properties with changing neutron number. The $Z = 50$ proton shell is closed, so one may assume that the low-lying states of these nuclei are predominantly formed by excitation of neutrons in the five active orbitals $0g_{7/2}$, $1d_{5/2}$, $1d_{3/2}$, $2s_{1/2}$, and $0h_{11/2}$.

Transfer reactions play an important role in our understanding of tin isotopes, since these reactions are very sensitive to the neutron structure of the isotopic sequence $N = 60$ (^{110}Sn) to $N = 76$ (^{126}Sn). In particular, two-neutron transfer reactions, such as (p, t), may be profitably used to provide detailed spectroscopic information for these nuclei and test the relative phases of spectroscopic amplitudes provided by shell-model wave functions.

In recent years, we have undertaken a systematic study of tin isotopes via (p, t) reactions in high-resolution experiments at the Munich HVEC MP Tandem. We reported the results for ^{122,116,112}Sn(p, t)^{120,114,110}Sn reactions in previous papers [1–3], where they were also compared with predictions of shell-model calculations. In this paper, we have extended our study to the ^{118}Sn nucleus via the ^{120}Sn(p, t)^{118}Sn reaction.

The level structure of ^{118}Sn has been studied by different kinds of experimental measurements: radioactivity studies from ^{118}In β decay (4.45 min [4], 5.0 s [5], and 8.5 s [6]), ^{118}Sb ϵ decay (3.6 min [7,8] and 5.00 h [8]), inelastic scattering of protons [9] and α particles [10], Coulomb excitation [11], in-beam γ-ray spectroscopy with both nonselective and selective reactions such as (n, $n'\gamma$) [12] and ^{116}Cd(α, $2n\gamma$)^{118}Sn [13,14] and ^{116}Cd(^{7}Li, $p4n\gamma$)^{118}Sn [15], respectively, and very sensitive and spin selective nuclear resonance fluorescence experiments [16].

The level scheme of ^{118}Sn has also been investigated using one-, two-, and four-nucleon transfer reactions: ^{117}Sn(d, p) ^{118}Sn [17], ^{119}Sn(p, d)^{118}Sn [18], ^{116}Sn(t, p) ^{118}Sn [19], ^{120}Sn(p, t) ^{118}Sn [20], and ^{122}Te(d,^{6}Li) ^{118}Sn [21]. In particular, two-neutron transfer reactions at low excitation energy, showing correlations arising from the pairing component of the interaction, characterize low-spin states and are therefore complementary to the (HI, $xn\gamma$) reactions. The fusion-evaporation reaction mechanism preferably feeds states with high alignment and is very selective in populating high-spin states.

TABLE I. Isotopic composition of the ^{120}Sn target.

Isotope	112	114	115	116	117	118	119	120	122	124
Percentage	<0.10	<0.01	<0.05	0.02	0.02	0.11	0.14	99.6	0.09	0.02

The results obtained in these studies are reported in the Nuclear Data Sheets (NDS) compilation [22], where a more complete list of references can be found.

Fleming *et al.* [20] first studied the ^{120}Sn$(p,t)^{118}$Sn reaction at an incident energy of 20 MeV in an experiment involving several other even Sn isotopes. For ^{118}Sn, only the cross sections of the 11 most intense (p,t) transitions were measured, with an energy resolution of 25 keV. This was the motivation for our new study of the ^{120}Sn$(p,t)^{118}$Sn reaction, performed in a high-resolution experiment at 21 MeV incident energy.

Accurate measurements of the differential cross sections for 38 transitions to final states of ^{118}Sn up to an excitation energy of 3.597 MeV, including a triplet and two doublets, allowed us to determine the angular momentum transfer to 42 levels and assign spin and parity to each of them. Very weakly populated states, with a lower limit for the integrated cross sections of only 0.8 μb, were also identified.

For a better understanding of ^{118}Sn, the present (p,t) experimental data have been supplemented by a shell-model study, which makes use of a two-body effective interaction derived from the CD-Bonn free nucleon-nucleon potential [23]. The doubly-magic nucleus ^{132}Sn is assumed to be a closed core, with the 14 valence neutron holes occupying the five levels of the 50–82 shell. Within this model space, the calculations are performed by employing the seniority scheme, including states with seniority up to 4.

We also perform microscopic distorted-wave Born approximation (DWBA) calculations of the (p,t) transfer, by using a simple one-step transfer theory [24,25] with ^{120}Sn ground-state and ^{118}Sn final-state wave functions generated by our shell-model calculation. Preliminary results of the present study were published in Ref. [26].

The setup and the experiment are described in the next section and the analysis of the experimental results is presented in Sec. III. Section IV is devoted to the theoretical analysis: In Sec. IV A we briefly outline the theoretical framework of our shell-model calculations and compare experimental and theoretical energy spectra; in Sec. IV B we show how form factors are derived in the microscopic DWBA calculation and compare experimental and theoretical cross-section angular distributions. A summary of our study is given in Sec. V.

II. THE EXPERIMENT

The ^{120}Sn$(p,t)^{118}$Sn reaction has been studied by using the 21-MeV proton beam delivered by the HVEC MP Tandem accelerator of the Maier-Leibnitz Laboratory of LMU Munich and the Technical University of Munich. The ^{120}Sn target, whose isotopic enrichment is reported in Table I, had a thickness of 114 μg/cm^2 on a carbon backing of 6 μg/cm^2. The high isotopic enrichment of the target enabled us to measure triton spectra free of contributions from different tin isotopes.

The beam current intensity was up to 500 nA and was integrated into a Faraday cup set behind the target.

The reaction products were momentum separated by the Q3D spectrograph and detected in its focal plane at 11 angles from 10° to 65° with respect to the beam axis in three different magnetic field settings up to an excitation energy of the ^{118}Sn residual nucleus of 3.597 MeV. The magnetic field values have been set to allow overlaps in energy.

The acceptance opening of the magnetic spectrograph was 11.04 msr (horizontal × vertical of 20 × 20 mm) for $\theta \geqslant 10°$.

The analyzed particles were detected in a 1.8-m-long focal plane detector [27] that consists of an array of single-wire proportional detectors with an additional cathode readout structure, followed by a rest energy plastic scintillator detector for particle identification. This device provides focal plane reconstruction, ΔE-E identification, and the position with good resolution. Because of the excellent separation of the tritons from other reaction products, the measured spectra are virtually free of contaminants: The spectrograph is an ideal instrument for the measurement of transfer reaction products. The excellent energetic characteristics of the accelerator, the Q3D, and the detector enable us to measure high-resolution excitation spectra, with an energy resolution of about 8 keV full width at half maximum in the detection of the outgoing tritons.

The energy calibration of the spectra of the ^{120}Sn$(p,t)^{118}$Sn reaction has been carried out by using a third-order polynomial. The polynomial parameters were set by reproducing well-known excitation energies of levels of ^{118}Sn determined in γ-decay experiments [22]. Our quoted energies are estimated at 3 keV.

Absolute cross sections have been determined with an uncertainty of ∼15%, by taking into account effective target thickness, solid angle, and collected charge.

The triton spectra were analyzed by means of the computer code AUTOFIT [28], with the shape of the triton peak at 2.734 MeV used as reference.

The high resolving power of the Q3D, the very low background, the large solid angle, the favorable peak to background ratio, and the spectrum energy resolution allowed measurement of rather weakly populated levels having cross-section values less than 0.3 μb/sr at the maximum of the angular distribution (see as an example the case of 2.999-MeV level).

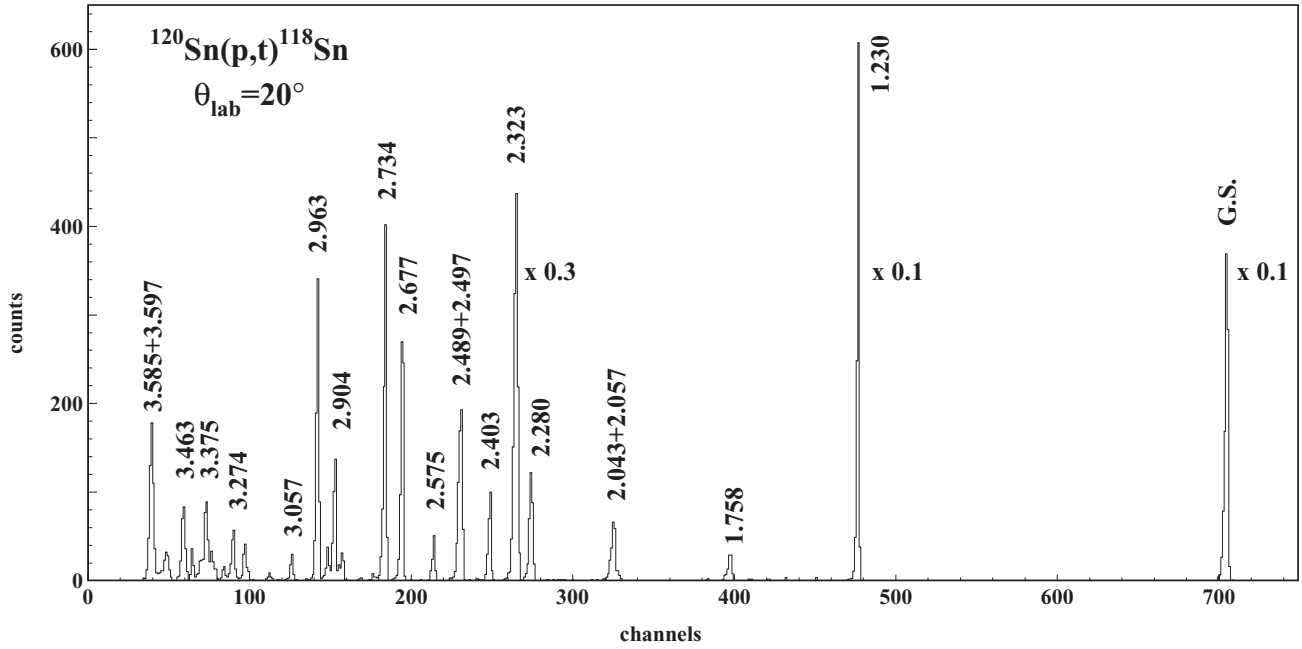

FIG. 1. Position spectrum of tritons measured at $\theta = 15^\circ$. Some levels are labeled with their excitation energy in MeV.

In Fig. 1 the measured triton spectrum at 20° is shown and the excitation energies of the most populated levels are indicated.

We have measured 38 transitions to the final states of ^{118}Sn up to $E_x = 3.597$ MeV; 5 of these have been observed for the first time.

The angular momentum transferred, the spin values, and the parity have been assigned by means of the cluster DWBA analysis reported in Sec. III.

Table II summarizes the results obtained in the present experiment: The energies, spins, and parities of the ^{118}Sn levels adopted so far are listed together with the energies, spins, and parities [22] observed in the present study of ^{120}Sn$(p, t)^{118}$Sn reaction. The integrated experimental cross sections, estimated with a systematic error of 15%, are also reported in the last column of Table II, together with the statistical errors.

III. ANALYSIS OF THE EXPERIMENTAL RESULTS

A direct one-step (p, t) transfer reaction on an even-even 0^+ target nucleus populates only natural parity states of the residual nucleus, with a unique L-transfer value, in the hypothesis that the two neutrons are transferred with a relative angular momentum of zero. In this case spin and parity of the observed levels are directly and unambiguously given by the assignment of the L transfer $[J_f = L, \pi_f = (-1)^L]$.

Initially a DWBA analysis of the experimental data concerning the ^{120}Sn$(p, t)^{118}$Sn reaction has been performed by assuming a semimicroscopic dineutron cluster pickup mechanism. The calculations have been carried out in a finite-range approximation, using the computer code TWOFNR [29] and following the same lines of those performed in the case of ^{114}Sn [2] and ^{112}Sn [3]. Basically we assume that the relative motion of the transferred spin-singlet neutron pair has zero orbital angular momentum and no radial nodes. The wave function of the center of mass of the transferred neutron pair is represented by a single-particle wave function with angular momentum equal to the total angular momentum L of the transferred pair. The number of nodes of the center-of-mass radial wave function is given by the conservation rule for three-dimensional harmonic oscillator quanta,

$$Q = 2N + L = \sum_{i=1}^{2} (2n_i + \ell_i),$$

where n_i and l_i are the quantum numbers of the individual shell-model states that form the transferred pair.

The angular distributions display shapes characteristic of the transferred angular momentum L and are only slightly affected if N changes by one, and they depend very little on the detailed microscopic shell-model components of the transferred dineutron cluster. Therefore cluster DWBA calculations represent a valid means in the use of the shape of the experimental angular distribution to extract the transferred angular momentum L. However, the details of the shell-model structure of the transferred cluster (i.e., n_i and l_i values of the cluster components and their relative phases) are of considerable importance in calculating the magnitude of the transfer cross section, as will be shown in Sec. IV B.

A proton-dineutron interaction potential of Gaussian form $V(r_{p2n}) = V_0 \exp[-(r_{p2n}/\xi)^2]$ with $\xi = 2$ fm has been used. The parameters for the proton entrance channel have been deduced from a systematic survey of elastic scattering by Perey [30] and for the triton exit channel by Fleming [20]. Table III summarizes the optical model parameters for the proton and triton elastic scattering, used in the Woods-Saxon parametrization and the geometric parameters for evaluating the bound-state wave function of the transferred dineutron

TABLE II. The adopted energies, spins, and parities [22] of the ^{118}Sn levels (columns 1 and 2), the energies, spins, and parities observed in the present work (columns 3 and 4), and the integrated cross sections from 7.5°(12.5° for the 2.999-MeV level) to 67.5° (column 5). Our quoted energies are estimated to have an uncertainty of ±3 keV. In column 5 absolute cross sections, estimated with a systematic error of ±15%, are reported together with the statistical errors.

Adopted		Present experiment		
E_{exc} (keV)	J^π	E_{exc} (MeV)	J^π	σ_{int} (μb)
0.0	0^+	0.0	0^+	2250 ± 14
1229.666	2^+	1.230	2^+	613 ± 12
1758.31	0^+	1.758	0^+	32 ± 2
2042.882	2^+	2.043	2^+	13 ± 1
2056.91	0^+	2.057	0^+	33 ± 2
2120	(2^+)			
2280.342	4^+	2.280	4^+	28 ± 2
2321.23	5^-			
		2.323	$5^- + 3^- + 2^+$	415 ± 6
2324.846	3^-			
2328.02	2^+			
2403.22	2^+	2.403	2^+	16 ± 1
2408	4^+			
2488.871	4^+	2.489	4^+	71 ± 2
2496.88	0^+	2.497	0^+	20 ± 1
2530				
2574.91	7^-	2.575	7^-	25 ± 1
2577	2^+			
2677.35	2^+	2.677	2^+	44 ± 2
2725	$1^+, 2^+, 3^+$			
2733.789	4^+	2.734	4^+	119 ± 3
2738.01	1^+			
2773.94	4^-			
2817	$(4^-, 5^-, 6^-)$			
2817.17	(3^-)			
2878.70	$4,5,6^+$	2.879	5^-	8 ± 1
2889	(8^+)			
2903.87	2^+	2.904	2^+	25 ± 1
2929.72	$0^+, 1^+$	2.930	0^+	10 ± 1
2934	(2^+)			
2963.437	4^+			
		2.963	5^-	115 ± 3
2972	4^+			
2991				
2999.45	6^+	2.999	6^+	0.8 ± 0.2
3015.21	1, 2, 3			
3020	0^+			
3048.35	4			
3052.16	$7^+, 8^+$			
3057.22	2^+	3.057	2^+	6 ± 1
3089.21	$^+$			
3108.06	$9^+, 10^+$			
		3.108	7^-	1 ± 0.3
3137.48	0^+	3.137	0^+	3 ± 1
3159.35	4^+			
3190				
		3.218	0^+	7 ± 1
3227.67	$2^+, 3^+$			
3228.37	2^+	3.228	2^+	6 ± 1
3231	(8^+)			
3237		3.237	0^+	1 ± 0.5
3252.03	(3^+)	3.252	6^+	4 ± 1
3262.53	3^+			
3270.67	1			
3274		3.274	$1^- + 3^-$	15 ± 1
3286				
3308.54	2^+			
		3.309	$1^- + 2^+$	6 ± 1
3317	$0^-, 1^-, 2^-$			
3344	(3^-)	3.344	3^-	8 ± 1
3355.86	2^+			
		3.355	0^+	12 ± 1
3363	$0^+, 1^+$			
3374.60	4^+			
		3.375	5^-	38 ± 2
3386.30	3^+			
3389				
		3.395	5^-	7 ± 1
3409				
3427.11	3^+			
		3.427	3^-	9 ± 1
3441				
3460.49	4^+			
3462.63	$(2^-, 3^-)$	3.463	2^+	19 ± 1
3475				
		3.524	2^+	9 ± 1
3540.57	$1^+, 2^+, 3^+$			
3541	$(6^+, 7^-)$	3.541	3^-	4 ± 1
3558.9	$7^-, 8^-, 9^-$			
		3.559	6^+	5 ± 1
3576	$2^-, 3^-, 4^-$			
		3.585	2^+	43 ± 2
3592.54	4^+			
3597	2^+	3.597	2^+	10 ± 1

cluster. These optical model parameters have been also used to analyze the angular distributions of the ^{122}Sn$(p,t)^{120}$Sn reaction measured at 20 MeV [20] and 26 MeV [1,31], the ^{116}Sn$(p,t)^{114}$Sn reaction measured at 26 MeV [2], the ^{112}Sn$(p,t)^{110}$Sn reaction measured at 26 MeV [3], and the ^{123}Sb$(p,t)^{121}$Sb reaction measured at 26 MeV [32], giving good agreement between experimental results and cluster DWBA calculations. Good agreement between experimental results and cluster DWBA calculations has been also achieved for the present ^{120}Sn$(p,t)^{118}$Sn reaction, allowing the assumption that multistep processes are relatively unimportant for this reaction. Thus, multistep processes are not taken into account in the present cluster DWBA analyses.

We have assigned the transferred L values, and consequently spins and parities of levels of the residual nucleus ^{118}Sn, by means of the comparison between the shapes of

TABLE III. The Woods-Saxon optical model parameters for the incident proton, the outgoing triton, and the geometrical parameters for the bound state of the transferred dineutron cluster.

	V_r (MeV)	r_r (fm)	a_r (fm)	W_v (MeV)	r_v (fm)	a_v (fm)	W_d (MeV)	r_d (fm)	a_d (fm)	V_{so} (MeV)	r_{so} (fm)	a_{so} (fm)	r_c (fm)
p	50.0	1.25	0.65				10.0	1.30	0.60	3.00	1.25	0.70	1.25
t	176.0	1.14	0.72	18.0	1.61	0.82				8.00	1.10	0.80	1.30
bound state		1.30	0.50										

the experimental angular distributions and the calculated ones, owing to their pronounced structure and difference for different L transfers. The 0^+ states are shown in Fig. 2; the 2^+ states in Fig. 3; the 4^+ and 6^+ states in Fig. 4; and the 3^-, 5^-, and 7^- states in Fig. 5. The 2.323-MeV triplet and the two doublets at 3.274 and 3.309 MeV are displayed in Fig. 6. In these figures the angular distributions for the observed levels are compared with the cluster DWBA calculations. For the triplet and doublets the percentage of the different L contributions have been determined by imposing the lowest value of χ^2.

As Table II shows, we have made spin-parity assignments for all the observed levels. In particular, with respect to the adopted levels (NDS) [22], 18 confirmations and 14 new assignments have been made and 6 ambiguities have

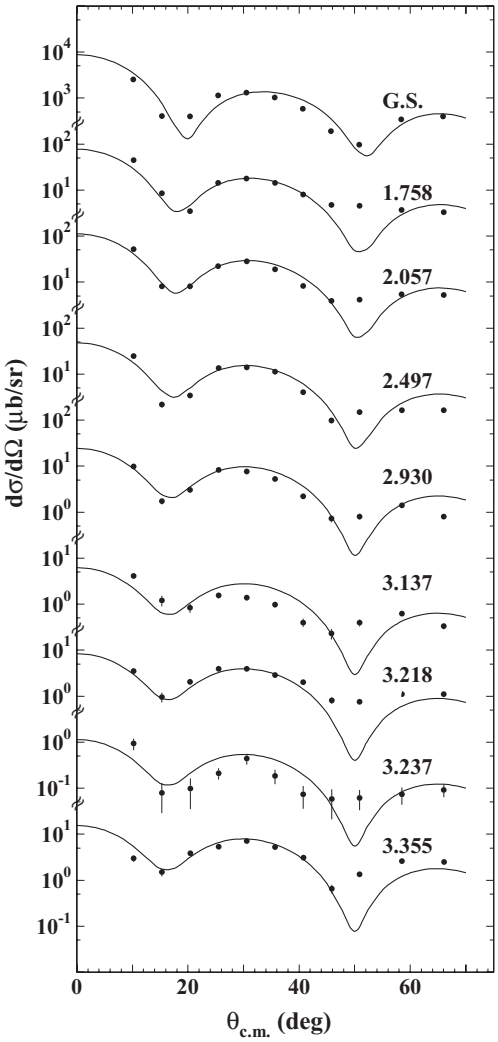

FIG. 2. Differential cross sections for the excitation of 0^+ states by the ^{120}Sn$(p, t)^{118}$Sn reaction. The dots represent the experimental data; the solid lines are the theoretical estimates obtained with semimicroscopic DWBA calculations. The energies attributed to the observed levels are those given in the present work.

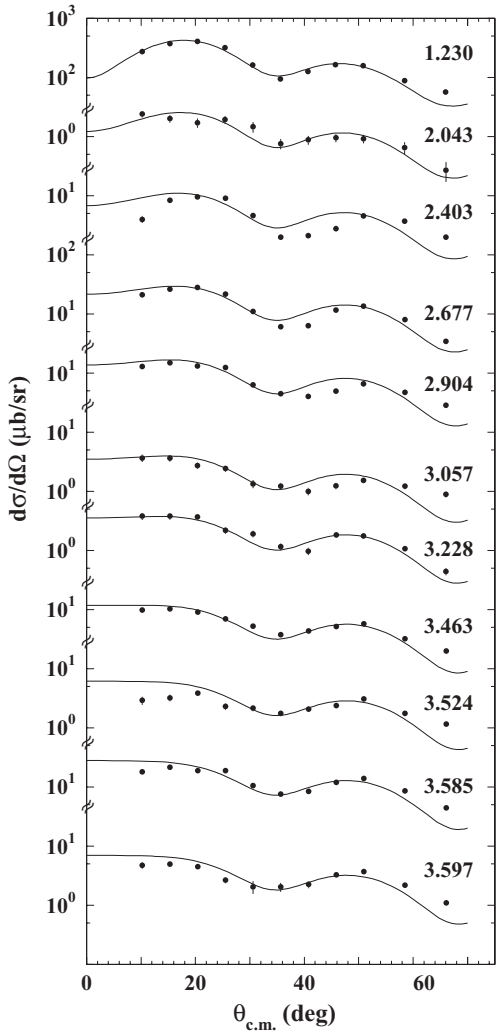

FIG. 3. Differential cross sections for the excitation of 2^+ states by the ^{120}Sn$(p, t)^{118}$Sn reaction. The dots represent the experimental data; the solid lines are the theoretical estimates obtained with semimicroscopic DWBA calculations. The energies attributed to the observed levels are those given in the present work.

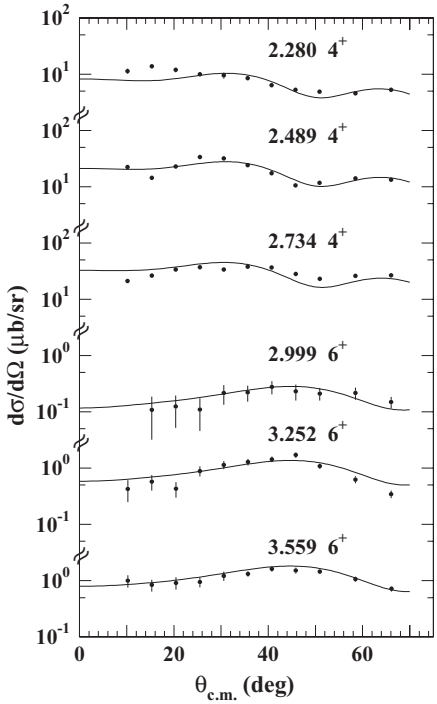

FIG. 4. Differential cross sections for the excitation of the three observed 4^+ and the three observed 6^+ states by the ^{120}Sn$(p, t)^{118}$Sn reaction. The dots represent the experimental data; the solid lines are the theoretical estimates obtained with semimicroscopic DWBA calculations. The energies attributed to the observed levels are those given in the present work.

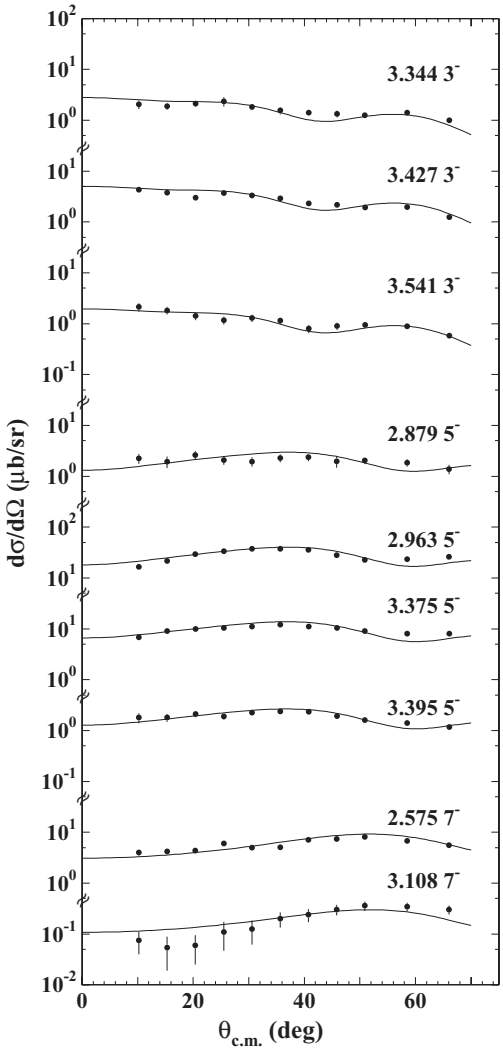

FIG. 5. Differential cross sections for the excitation of the three observed 3^-, the four observed 5^-, and the two observed 7^- states by the ^{120}Sn$(p, t)^{118}$Sn reaction. The dots represent the experimental data; the solid lines are the theoretical estimates obtained with semimicroscopic DWBA calculations. The energies attributed to the observed levels are those given in the present work.

been removed. Two unresolved doublets and one triplet have been also observed, giving six confirmations and one new assignment. The proposed assignments for the levels identified in the present experiment that are new or correspond to those reported in the NDS [22] with uncertain J^π or without J^π assignment are discussed in the following, together with the assignments of the unresolved triplet and doublets. The four removed ambiguities concern the 2.879-, 2.930-, 3.344-, and 3.463-MeV levels.

(i) 2.323 MeV: The NDS [22] report three levels, the first at 2321.23 keV with $J^\pi = 5^-$ from ^{118}In β^- decay (8.5 s) and from ^{118}Sb ϵ decay (5 h) [6] studies and from a ^{118}Sn$(n, n'\gamma)$ study [12], the second at 2324.846 keV with $J^\pi = 3^-$ from a ^{118}Sn$(n, n'\gamma)$ study [12], and the third at 2328.02 keV with $J^\pi = 2^+$ from a ^{118}Sn$(n, n'\gamma)$ study [12]. In our measurement this transition is quite strongly populated and the shape of the angular distribution is well reproduced by an unresolved triplet with $J^\pi = 5^-(33\%)$, $J^\pi = 3^-(33\%)$, and $J^\pi = 2^+(33\%)$.

(ii) 2.879 MeV: In the adopted level scheme [22] a level is reported at 2878.70 keV with $J^\pi = 4, 5, 6^+$. The J^π assignment is deduced from a study concerning ^{118}In β^- decay (4.45 min) [4], which suggests a value of $J^\pi = (5^-)$, and from a measurement of the ^{116}Cd$(\alpha, 2n\gamma)$ reaction [14] with $J^\pi = (6^+)$. A ^{118}Sn$(n, n'\gamma)$ study [12] assigns $J^\pi = 5^-, (6^+)$. Our measured angular distribution is well reproduced by assuming $L = 5$ transfer. The present assignment $J^\pi = 5^-$ removes the ambiguity.

(iii) 2.930 MeV: Two levels are reported in the NDS [22], the first at 2929.72 keV with $J^\pi = 0^+, 1^+$ and the second at 2934 keV with $J^\pi = (2^+)$. For the level at 2929.72 keV the J^π assignment is deduced on the basis of a study of ^{117}Sn(d, p) [17] that identifies an angular momentum transfer $L = 0$ and a study of ^{118}Sn$(n, n'\gamma)$ [12] that assigns $J^\pi = (0^+)$. For the level at 2934 keV, the $J^\pi = (2^+)$ assignment is based on an $L = (2)$ transfer in a (p, p') study [9]. The angular distribution for the level at 2.930 MeV displays a very steeply rising cross section at small reaction angles and a

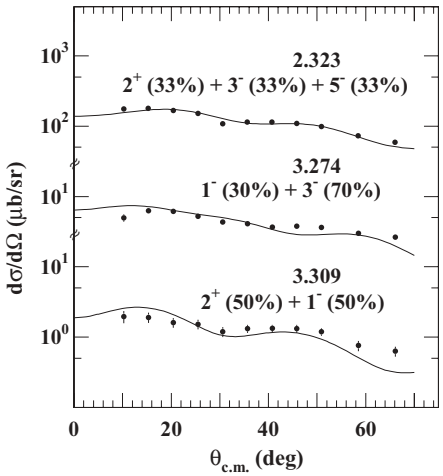

FIG. 6. Differential cross sections for the excitation of the triplet at 2.323 MeV and the two doublets at 3.274 and 3.309 MeV observed by the ^{120}Sn$(p, t)^{118}$Sn reaction. The dots represent the experimental data; the solid lines are the theoretical estimates obtained with semimicroscopic DWBA calculations. The energies attributed to the observed levels are those given in the present work.

sharp minimum at the detector angle of about 20°. This pattern is typical of $L = 0$ transfer and is well reproduced by our calculated 2.930-MeV angular distribution. This corresponds to the 2929.72-keV level, and our assignment is $J^\pi = 0^+$.

(iv) 2.963 MeV: The shape of the angular distribution of this strongly populated level is quite well reproduced by $L = 5$ transfer. The assignment of spin and parity is consequently $J^\pi = 5^-$. Probably this level cannot coincide with the level reported in the NDS [22] at 2963.437 keV with $J^\pi = 4^+$ from ^{118}Inβ^- decay (4.45 min) [4] and ^{118}Sn$(n, n'\gamma)$ [12] and ^{118}Sn(α, α') [10] studies.

(v) 3.108 MeV: In our experiment this level is quite weakly populated, the cross section at the maximum in the angular distribution being about 0.35 μb/sr. An $L = 7$ transfer reasonably reproduces the angular distribution. The present assignment is $J^\pi = 7^-$. The adopted level scheme [22] reports a level at 3108.6 keV with $J^\pi = 9^+, 10^+$. From the ^{116}Cd$(\alpha, 2n\gamma)$ reaction [14] this level is identified as $J^\pi = 10^+$. The level we find at 3.108 MeV presumably does not coincide with the 3108.06-keV level.

(vi) 3.218 MeV: The transition to this level is observed to exhibit an angular distribution with $L = 0$ shape. The J^π assignment is therefore 0^+. In the NDS [22] no level is given at this energy.

(vii) 3.237 MeV: In the NDS [22] a level is reported without spin and parity attribution at this energy on the basis of ^{117}Sn(d, p) [17] and ^{118}Sn(p, p') [33] reactions. In the present experiment the level at 3.237 MeV is weakly populated and the angular distribution is compatible with an $L = 0$ transfer. The present assignment is 0^+.

(viii) 3.252 MeV: In Ref. [22] a level is denoted with an energy of 3252.03 keV and $J^\pi = (3^+)$. The ^{118}Sn$(n, n'\gamma)$ study [12], based on $\gamma(\theta)$ and γ linear polarization, suggests $J^\pi = 2, 3^+$. In our case the 3.252-MeV level angular distribution is consistent with an attribution of $J^\pi = 6^+$.

(ix) 3.274 MeV: In the NDS [22] two levels are reported, one at 3270.67 keV with $J = 1$ derived from an $(n, n'\gamma)$ study [12] and another at 3274 keV without spin and parity assignment derived from ^{117}Sn(d, p) [17]. We reproduce the observed angular distribution quite well by considering an unresolved doublet with $J^\pi = 1^-$ (30%) and $J^\pi = 3^-$ (70%).

(x) 3.309 MeV: The NDS [22] report two levels, the first at 3308.54 keV with $J^\pi = 2^+$ observed in the $(n, n'\gamma)$ reaction [12] and the second at 3317 keV with $J^\pi = 0^-, 1^-, 2^-$ deduced from a ^{117}Sn(d, p) reaction study [17]. The angular distribution shape is reproduced by considering an unresolved doublet with $J^\pi = 2^+$ (50%) and $J^\pi = 1^-$ (50%).

(xi) 3.344 MeV: The NDS [22] report with a tentative $J^\pi = (3^-)$ from a ^{118}Sn(p, p') reaction study [9]. In that study an $L = (3)$ transfer is assumed. In our measurement we reproduce quite well the differential cross section considering an $L = 3$ transfer. The present assignment is $J^\pi = 3^-$.

(xii) 3.355 MeV: In the NDS [22] two levels are given, one with an energy 3355.86 keV with spin and parity attribution of 2^+ resulting from the ^{118}Sn$(n, n'\gamma)$ study [12] and another from a ^{117}Sn(d, p) reaction study [17] at (3363 ± 3) keV with $J^\pi = 0^+, 1^+$. In our case the 3.355-MeV level angular distribution displays a characteristic $L = 0$ transfer shape. The present assignment is $J^\pi = 0^+$.

(xiii) 3.375 MeV: The transition populating this level is well reproduced by an $L = 5$ transfer. The present assignment is $J^\pi = 5^-$. Therefore, this level might not correspond to the adopted level [22] reported at 3374.60 keV with $J^\pi = 4^+$ from a study of ^{118}Inβ^- decay (4.45 min) [4].

(xiv) 3.395 MeV: The adopted scheme [22] does not give any level at this energy. In our measurement, the differential cross section is quite accurately reproduced by assuming an $L = 5$ transfer. The J^π attribution is 5^-.

(xv) 3.427 MeV: The spin and parity reported in the NDS [22] for the level at 3427.11 keV are 3^+. The ^{118}Sn$(n, n'\gamma)$ study [12] gives $J^\pi = (2^+), 3$. We accurately reproduce the measured angular distribution shape by assuming an $L = 3$ transfer for the transition to the level. The present assignment is $J^\pi = 3^-$.

(xvi) 3.524 MeV: In the NDS [22] no level is reported at this energy. The measured differential cross section is compatible with an attribution of $J^\pi = 2^+$.

(xvii) 3.541 MeV: The adopted level scheme [22] reports two levels,k one at 3540.57 keV with $J^\pi = 1^+, 2^+, 3^+$ identified in the ^{117}Sn(d, p) reaction study [17] with $L = (2)$ transfer and in ^{119}Sn(p, d) [18] with $L = 2$ transfer and the the other at (3541 ± 10) keV in a

(p, p') study with $L = (6, 7)$ transfer [9]. In the present experiment the angular distribution is consistent with $L = 3$ transfer and our assignment is $J^\pi = 3^-$.

(xviii) 3.559 MeV: In the NDS [22] a level is reported at 3558.9 keV with $J^\pi = 7^-, 8^-, 9^-$ identified in a study of ^{118}Sb ϵ decay (5 h) [6]. In our case the observed level is weakly populated and we nicely reproduce the measured angular distribution with $L = 6$ transfer. The present assignment is $J^\pi = 6^+$.

(xix) 3.585 MeV: The NDS [22] do not report a level at this energy. In our case the level is reasonably populated, and an $L = 2$ transfer satisfactory reproduces the measured angular distribution. The assignment is $J^\pi = 2^+$.

(xx) 3.597 MeV: The adopted level scheme [22] reports a level at 3597 keV with $J^\pi = 2^+$ identified as $L = 2$ transfer in a (p, p') study [9] and in a ^{117}Sn(d, p) reaction study [17]. We nicely reproduce the measured angular distribution with an $L = 2$ transfer. The present assignment is $J^\pi = 2^+$.

IV. THEORETICAL ANALYSIS

A. Shell-model calculations

Our shell-model study of ^{118}Sn is based on the use of a realistic two-body effective interaction, as were our previous studies of ^{110,114,120}Sn [1–3]. As in our paper on ^{110}Sn [3], this interaction is derived from the CD-Bonn nucleon-nucleon potential [23] whose repulsive core is renormalized by constructing a low-momentum potential $V_{\mathrm{low}\,k}$ defined up to a cutoff momentum of 2.1 fm^{-1} [34]. This $V_{\mathrm{low}\,k}$ is a smooth potential that can be used directly as input in the $\hat{Q}$-box folded-diagram expansion [35] for the calculation of the shell-model effective interaction.

We start by assuming ^{132}Sn as a closed core, with the 14 valence neutron holes occupying the five levels $0g_{7/2}$, $1d_{5/2}$, $1d_{3/2}$, $2s_{1/2}$, and $0h_{11/2}$ of the 50–82 shell. As a first step, we calculate the $\hat{Q}$-box, including diagrams up to second order in $V_{\mathrm{low}\,k}$. The computation of these diagrams is performed within an harmonic-oscillator basis by using intermediate states composed of particle and hole states restricted to the two major shells above and below the $Z = 50$, $N = 82$ Fermi surface. The oscillator parameter is $\hbar\omega = 7.88$ MeV, as obtained from the expression $\hbar\omega = 45A^{-1/3} - 25A^{-2/3}$. As a final step, the effective interaction is obtained by summing the $\hat{Q}$-box folded-diagram series to all orders by means of the Lee-Suzuki iteration method [36].

It is worth noting that in the present calculation for 14 valence holes inside ^{132}Sn, we need hole-hole matrix elements of the effective interaction. Their calculation is somewhat different from that for particles as regards the computation of the $\hat{Q}$-box diagrams. This is shown in Ref. [37].

We should also mention that we have made no attempt to modify empirically the interaction obtained by following this procedure, which is appropriate for the two-hole system. However, to account partially for correlations that set in as we move away from closed shells, we have determined the five single-hole (SH) levels through a fit to the yrast states of ^{119}Sn with the corresponding angular momentum and parity (instead of taking them from the experimental spectrum of ^{131}Sn).

Our adopted values are (in MeV) $\epsilon^{-1}_{g_{7/2}} = 2.8$, $\epsilon^{-1}_{d_{5/2}} = 2.155$, $\epsilon^{-1}_{s_{1/2}} = 0.85$, $\epsilon^{-1}_{d_{3/2}} = 1.2$, and $\epsilon^{-1}_{h_{11/2}} = 0.0$.

Having determined the one- and two-body terms of the Hamiltonian, we can calculate the energy spectrum of ^{118}Sn, as well as the spectroscopic amplitudes needed to compute the differential cross sections, as shown in Sec. IV B. This has been performed by using the chain-calculation method (CCM) described in Refs. [1,38], which is an approach to shell-model calculations based on the seniority scheme. As mentioned in the Sec. I, we have included here states with seniority $v \leqslant 4$, as was done in our previous studies of ^{114}Sn [2] and ^{120}Sn [1].

TABLE IV. Comparison of calculated energies with those obtained from the present experiment. See text for details.

J^π	E_{calc} (MeV)	E_{expt} (MeV)	J^π	E_{calc} (MeV)	E_{expt} (MeV)
0^+	0.000	0.000	4^+	2.564	2.280
	1.805	1.758		2.855	2.489
	2.090	2.057		3.198	2.734
	3.077	2.497			
	3.385	2.930	6^+	2.900	2.999
	3.700	3.137		3.856	3.252
	3.946	3.218		4.153	3.559
	4.215	3.237			
	4.262	3.355	5^-	2.427	2.323
				2.728	2.879
2^+	1.641	1.230		3.218	2.963
	2.483	2.043		3.388	3.375
	2.502	2.323		3.720	3.395
	2.895	2.403			
	3.181	2.677	7^-	2.546	2.575
	3.275	2.904		3.245	3.108
	3.449	3.057			
	3.633	3.228			
	3.799	3.309			
	3.938	3.463			
	4.039	3.524			
	4.228	3.585			
	4.201	3.597			

In Table IV, the excitation energies measured in the present experiment are compared with the calculated ones. We have excluded the 3^- and 1^- states, for which the discrepancies between experiment and theory are very large. They are, in fact, above 1 MeV for the two observed 1^- states and above 2 MeV for the four 3^- states. The description of these states seems to be therefore beyond the scope of the present calculation, which is likely to be traced to the effects of configurations outside the chosen model space.

As a general remark, we note that for half of the states shown in Table IV the experimental energies are overestimated by more than 400 keV. This can be partly attributed to the lack of $v > 4$ components, whose inclusion should in principle

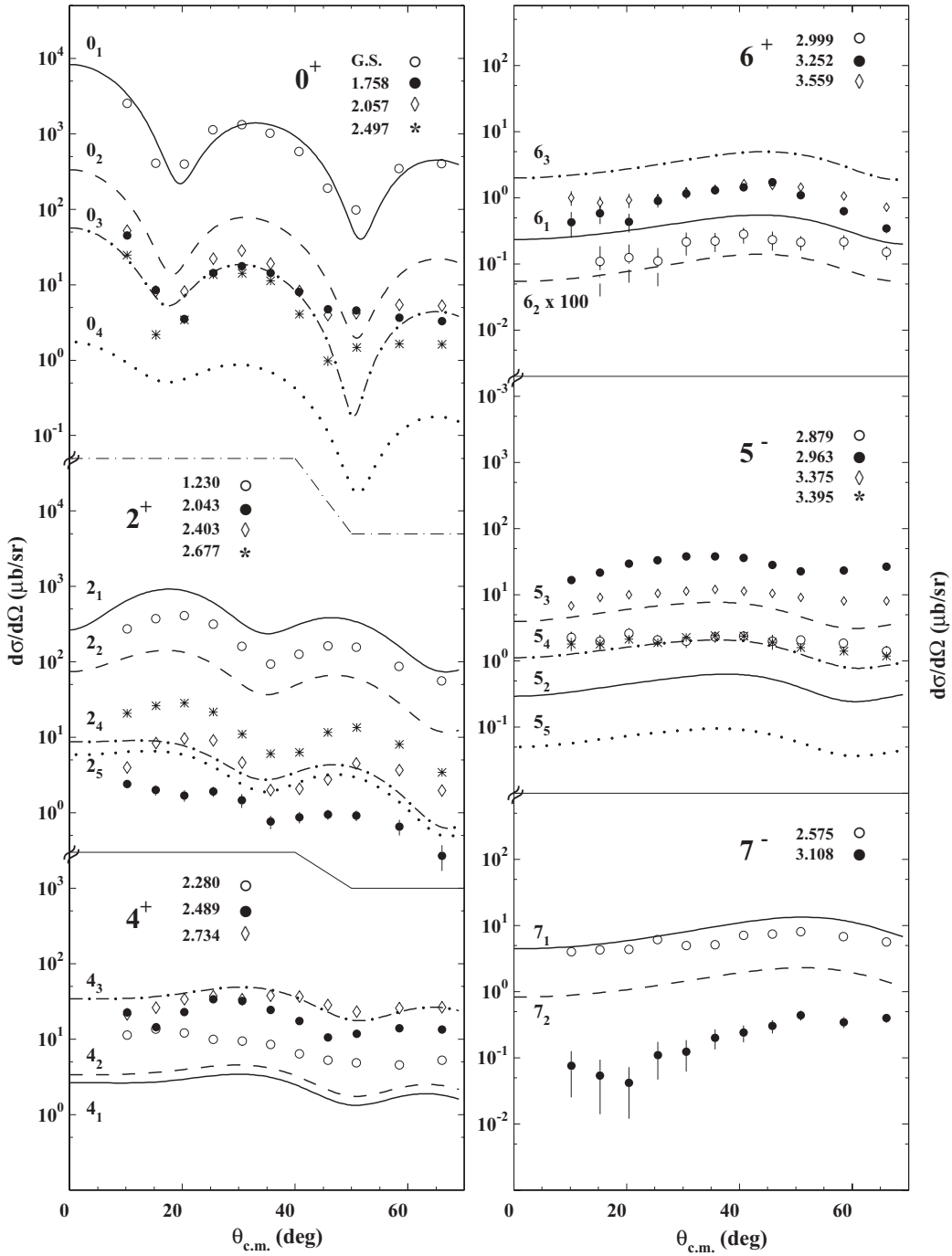

FIG. 7. Comparison between calculated and predicted differential cross sections for 0^+, 2^+, 4^+, 5^-, 6^+, and 7^- final states. The lines represent results of the microscopic calculations of the differential cross sections (in μb/ster) as a function of center-of-mass angle (in degrees). The subscripts 1, 2, 3, and 4 associated with the lines indicate the calculated energy ranking of the corresponding states, with 1 representing the lowest state of given J^π. Error bars are shown for the lowest 6^+ and 7^- states; in all other cases, the error bars are smaller than the symbol representing the measured differential cross section. Note that the data points correspond only to clearly resolved states. The (5^-, 3^-, 2^+) triplet at 2.323 MeV and the (1^-, 3^-) doublet at 3.274 MeV are not represented in the figure.

produce a downshift of most of the states. This is not expected, however, for the first 2^+ state. The energy of this state is also overestimated by our calculation in light tin isotopes [39] and in ^{110,114}Sn [2,3], although a full shell-model basis was used for the former and for ^{110}Sn. However, it is worth noting that the energies of the second and third 0^+ states in ^{118}Sn are well reproduced by the theory, at variance with what happens in ^{110,114}Sn. A reasonably good agreement between theory and

experiment is also obtained for all reported negative-parity states, with the discrepancies ranging from a few tens of keV to about 350 keV.

B. Microscopic DWBA calculations

In this section we will attempt to determine whether the shell-model eigenstates of ^{120}Sn and ^{118}Sn, calculated by the procedure discussed in Sec. IV A, are consistent with the measured differential cross sections. This will require us to describe the two-neutron transfer process microscopically.

Our main assumption is that the reaction involves direct transfer, so that the only relevant degrees of freedom are those of the proton and the transferred neutrons. We do not include any compound nucleus effects, in which the outgoing triton is emitted long after the energy of the incoming proton is shared with many of the target nucleons. In the simplest version of direct two-neutron pickup it is assumed that the relative motion of the two neutrons is not changed during the transfer. Thus the only part of the target two-neutron wave function that contributes is the part where the two neutrons have the same relative motion that they will have in the outgoing triton, namely with zero relative orbital angular momentum and zero total intrinsic spin angular momentum.

The details of this reaction theory have been presented elsewhere (see Ref. [3] and further references given there). We give here a brief summary of the important steps in the calculation. Starting with the target wave function, two types of projection are required:

(i) One must project out the degrees of freedom of the target nucleons that are not involved in the transfer. What remains is the wave function of the transferred neutrons, in the form

$$\sum_{n_1,\ell_1,j_1;n_2,\ell_2,j_2} S^J_{n_1,\ell_1,j_1;n_2,\ell_2,j_2} \times \frac{[\psi^{n_1,\ell_1,j_1}(\mathbf{r}_1,\sigma_1)\psi^{n_2,\ell_2,j_2}(\mathbf{r}_2,\sigma_2)]^J_M - [\psi^{n_1,\ell_1,j_1}(\mathbf{r}_2,\sigma_2)\psi^{n_2,\ell_2,j_2}(\mathbf{r}_1,\sigma_1)]^J_M}{2(1+\delta_{n_1,n_2}\delta_{\ell_1,\ell_2}\delta_{j_1,j_2})}. \quad (1)$$

The $S^J_{n_1,\ell_1,j_1;n_2,\ell_2,j_2}$ coefficients entering in Eq. (1) are the spectroscopic amplitudes, which are calculated from the target and residual shell-model eigenstates. The $\psi^{n_i,\ell_i,j_i}_{m_i}(\mathbf{r}_i,\sigma_i)$ are single-neutron shell-model orbitals. Equation (1) exhibits the coherence of the components associated with the different transferred configurations, a characteristic of direct theories of multinucleon transfer.

(ii) One must project out the part of Eq. (1) in which the neutrons have the intrinsic spin and relative orbital motion that they will have in the outgoing triton. The result is a function of the position of the two-neutron mass center, $F(R)Y^J_M(\hat{\mathbf{R}})$, which serves as the form factor of a DWBA calculation. We used the DWBA program TWOFNR [29], with the optical parameters listed in Table III, the same optical parameters that were used in the cluster transfer calculation of Sec. III.

Because this theory uses a collective interaction between the proton and the transferred neutrons, rather than a realistic interaction between the proton and the individual neutrons, it is difficult to express the results in terms of absolute differential cross sections. However, the relative differential cross sections at different outgoing triton angles, and between different final states of the residual nucleus, should be adequately described by the theory. Therefore, in the presentation of the results of the calculation, we have normalized the calculated differential cross section with a single multiplicative factor, chosen to give the best visual fit to the measured ground-state (0^+_1) angular distribution. This single multiplicative factor was used for all final states. This is in contrast to the procedure followed in Sec. III, where each calculated angular distribution was normalized separately to give an approximate fit to the data. Our object there was to use the shapes of the angular distributions to assign L values to the transfers, not to test shell-model descriptions of individual final states.

Figure 7 summarizes the comparison between calculated and predicted differential cross sections for 0^+, 2^+, 4^+,

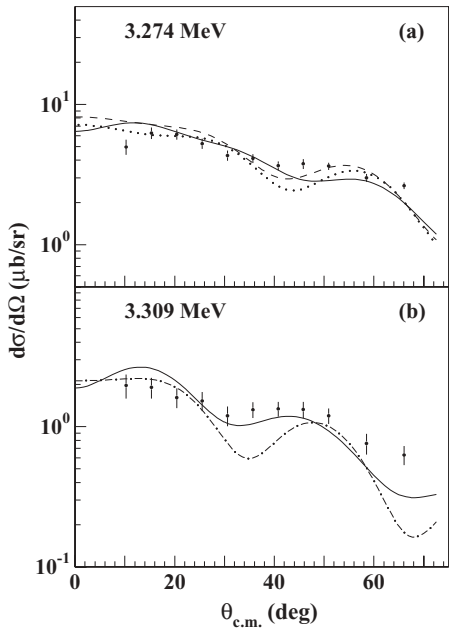

FIG. 8. Comparison of measured differential cross sections with calculations based on assumed L^π transfers, or mixtures of assumed L^π transfers. (a) 30% 1^-, 70% 3^- (solid line); 15% 2^+, 85% 3^- (dashed line); 100% 3^- (dotted line). (b) 50%1^-, 50%2^+ (solid line); 100% 2^+ (dot-dashed line).

5^-, 6^+, and 7^- final states. Note that the version of two-neutron-transfer theory that we use, in which the transferred neutrons have zero total spin and zero relative orbital angular momentum, predicts that only natural parity states will be populated. Therefore it is noteworthy that known unnatural parity states at 2738 keV (1^+), 2774 keV (4^-), and 3386 keV (3^+) do not appear in our observed (p, t) spectrum.

The most striking feature of the observed (p, t) spectrum is the dominance of the ground-state transition. For example, at 30° the ground-state transition is stronger than the 2_1^+ transition by a factor of 8 and stronger than any other transition by more than a factor of 35. This ground-state dominance is also exhibited by the results of the microscopic calculations, where the ground-state transition has about 4 times the strength of the 2_1^+ transition and about 50 times the strength of any other transition.

It is seen from Fig. 7 that the microscopic theory overpredicts the strength of the 2_1^+ transition, relative to the ground-state transition, by a factor of about 2. This may imply that the real 2_1^+ level has greater complexity than is afforded by the shell-model configurations we have included. If this more complex component of the real 2_1^+ level cannot be reached from the ^{120}Sn ground state by the (p, t), then the observed cross section would be lower than we would calculate on the basis of simple shell-model configurations.

The orders of magnitude of the strengths of the transitions to the odd-parity states are reasonably well accounted for, although we cannot claim level-by-level agreement. We have no predictions for transitions to 1^- states, because the single-neutron orbitals included in our shell-model calculation do not allow us to pick up a neutron pair coupled to 1^-. However, there is some evidence that we do populate 1^- states. For example, the NDS table reports a $J = 1$ level at 3270.67 keV, without a parity attribution, and a level at 3274 ± 3 keV, with neither a parity nor an angular momentum attribution. Figure 8(a) shows our measured angular distribution for this unresolved doublet, together with three cluster-transfer-calculated angular distributions. In our opinion, the best fit to the data is obtained for the mixed $L = 1$, $L = 3$ combination. Similarly, the NDS tables report a $J = 2^+$ level at 3308.54 keV and a $J = (0^-, 1^-, 2^-)$ level at 3317 ± 3 or 3310 ± 10 keV. Figure 8(b) shows that our measured angular distribution for the doublet at 3309 keV is better described by a 1^-, 2^+ admixture than by a pure 2^+ transition.

The properties of 1^- states in the ^{116,118,120,122,124}Sn isotopes have been discussed by Bryssinck *et al*. [16] in terms of $2^+ \otimes 3^-$ two-phonon excitations.

V. SUMMARY

The ^{120}Sn$(p, t)^{118}$Sn reaction has been studied in a high-resolution experiment at an incident proton energy of 21 MeV. We have measured differential cross sections for 38 transitions, including a triplet and two doublets, to levels of ^{118}Sn up to an excitation energy of 3.597 MeV. Spins and parities have been assigned to all the observed levels by carrying out a finite-range DWBA analysis in which a semimicroscopic dineutron cluster pickup mechanism was assumed. With respect to the adopted levels, 18 previous assignments have been confirmed, 14 new assignments have been made, and 6 ambiguities have been removed. The two unresolved doublets and the triplet give six confirmations and one new assignment.

Motivated by the present experiment, we have performed a shell-model study of ^{118}Sn with 14 neutron holes inside the ^{132}Sn core. The two-body matrix elements of the effective interaction have been derived from the CD-Bonn nucleon-nucleon potential, and the single-hole energies have been determined by reproducing the experimental energies of the yrast $J^\pi = 7/2^+, 5/2^+, 3/2^+, 1/2^+$, and $11/2^-$ states in ^{119}Sn. The calculations have been carried out within the seniority scheme, truncating the model space to states with $v \leqslant 4$. Experimental and theoretical energies are compared for the states identified in the present experiment, with the exception of 1^- and 3^- states for which the discrepancies are very large. Almost all experimental energies are overestimated by our calculation with discrepancies ranging from a few keV to 1 MeV. Good agreement is obtained for the negative-parity states.

A one-step microscopic DWBA calculation of differential cross sections has also been performed by using two-neutron spectroscopic amplitudes obtained from our shell-model calculations for ^{118}Sn and ^{120}Sn. The results reproduce the observed dominance of the ground-state transition although the quantitative agreement between experimental and theoretical differential cross sections cannot be considered completely satisfactory. In particular, we can account for the orders of magnitude of the strengths of transitions to odd-parity states, but we cannot claim level-by-level agreement.

[1] P. Guazzoni, M. Jaskóla, L. Zetta, A. Covello, A. Gargano, Y. Eisermann, G. Graw, R. Hertenberger, A. Metz, F. Nuoffer, and G. Staudt, Phys. Rev. C **60**, 054603 (1999).
[2] P. Guazzoni, L. Zetta, A. Covello, A. Gargano, G. Graw, R. Hertenberger, H.-F. Wirth, and M. Jaskóla, Phys. Rev. C **69**, 024619 (2004).
[3] P. Guazzoni, L. Zetta, A. Covello, A. Gargano, B. F. Bayman, G. Graw, R. Hertenberger, H.-F. Wirth, and M. Jaskóla, Phys. Rev. C **74**, 054605 (2006).
[4] S. Raman, T. A. Walkiewicz, L. G. Multhauf, K. G. Tirsell, G. Bonsignori, and K. Allaart, Phys. Rev. C **37**, 1203 (1988).
[5] D. De Frenne, H. Thierens, E. Jacobs, P. D'hondt, A. De Clercq, K. Heyde, and A. J. Deruytter, Phys. Rev. C **15**, 1440 (1977).
[6] J. Hattula, E. Liukkonen, and J. Kantele, Nucl. Phys. **A125**, 477 (1969).
[7] H. Kawakami, N. Yoshikawa, K. Komura, M. Koike, and H. Yamada, Phys. Rev. C **25**, 2013 (1982).
[8] J. Hattula, E. Liukkonen, and J. Kantele, Z. Phys. **231**, 203 (1970).
[9] O. Beer, A. El Behay, P. Lopato, Y. Terrien, G. Vallois, K. K. Seth, Nucl. Phys. **A147**, 326 (1970).
[10] G. Bruge, J. C. Faivre, H. Faraggi, and A. Bussiere, Nucl. Phys. **A146**, 597 (1970).

[11] N.-G. Jonsson, A. Backlin, J. Kantele, R. Julin, M. Luontama, and A. Passoja, Nucl. Phys. **A371**, 333 (1981).
[12] I. V. Mikhailov and A. M. Demidov, Izv. Akad. Nauk. SSSR, Ser. Fiz. **53**, 892 (1989) [Bull. Acad. Sci. USSR, Phys. Ser. **53**, 69 (1989)].
[13] J. Bron, W. H. A. Hesselink, A. Van Poelgeest, J. J. A. Zalmstra, M. J. Uitzinger, H. Verheul, K. Heyde, and M. Waroquier, Nucl. Phys. **A318**, 335 (1979).
[14] A. Van Poelgeest, J. Bron, W. H. A. Hesselink, K. Allaart, J. J. A. Zalmstra, M. J. Uitzinger, and H. Verheul, Nucl. Phys. **A346**, 70 (1980).
[15] S. Lunardi, P. J. Daly, F. Soramel, C. Signorini, B. Fornal, G. Fortuna, A. M. Stefanini, R. Broda, W. Meczynski, and J. Blomquist, Z. Phys. A **328**, 487 (1987).
[16] J. Bryssinck, L. Govor, D. Belic, F. Bauwens, O. Beck, P. von Brentano, D. De Frenne, T. Eckert, C. Fransen, K. Govaert, R.-D. Herzberg, E. Jacobs, U. Kneissl, H. Maser, A. Nord, N. Pietralla, H. H. Pitz, V. Yu. Ponomarev, and V. Werner, Phys. Rev. C **59**, 1930 (1999).
[17] E. Frota-Pessoa, Nuovo Cimento A **77**, 369 (1983).
[18] D. G. Fleming, Can. J. Phys. **60**, 428 (1982).
[19] J. H. Bjerregaard, O. Hansen, O. Nathan, L. Vistisen, R. Chapman, and S. Hinds, Nucl. Phys. **A110**, 1 (1968).
[20] D. G. Fleming, M. Blann, H. W. Fulbright, and J. A. Robbins, Nucl. Phys. **A157**, 1 (1970).
[21] J. Janecke, F. D. Becchetti, and C. E. Thorn, Nucl. Phys. **A325**, 337 (1979).
[22] K. Kitao, Nucl. Data Sheets **75**, 99 (1985).
[23] R. Machleidt, Phys. Rev. C **63**, 024001 (2001).
[24] B. F. Bayman and A. Kallio, Phys. Rev. **156**, 1126 (1967).
[25] D. N. Mihailidis, N. M. Hintz, A. Sethi, and E. J. Stephenson, Phys. Rev. C **64**, 054608 (2001).
[26] P. Guazzoni, L. Zetta, A. Covello, A. Gargano, B. F. Bayman, G. Graw, R. Hertenberger, T. Faestermann, H.-F. Wirth, and M. Jaskóla, *Changing Facets of Nuclear Structure,* in *Proceedings of the 9th International Spring Seminar on Nuclear Physics, Vico Equense, 2007*, edited by A. Covello (World Scientific, Singapore, 2008), p. 315.
[27] E. Zanotti, M. Bisenberger, R. Hertenberger, H. Kader, and G. Graw, Nucl. Instrum. Methods Phys. Res. A **310**, 706 (1991).
[28] J. R. Comfort, ANL Physics Division Informal Report No. PHY-1970 B, 1970 (unpublished).
[29] M. Igarashi, Computer code TWOFNR, 1977.
[30] F. G. Perey, Phys. Rev. **131**, 745 (1963).
[31] G. Cata-Danil, P. Guazzoni, M. Jaskóla, L. Zetta, G. Graw, R. Hertenberger, D. Hofer, P. Schiemenz, B. Valnion, E. Zanotti-Mueller, U. Atzrott, F. Hoyler, F. Nuoffer, and G. Staudt, J. Phys. G **22**, 107 (1996).
[32] P. Guazzoni, M. Jaskóla, V. Y. Ponomarev, L. Zetta, G. Graw, R. Hertenberger, and G. Staudt, Phys. Rev. C **62**, 054312 (2000).
[33] D. H. Allan, Nucl. Phys. **A114**, 211 (1968).
[34] S. Bogner, T. T. S. Kuo, L. Coraggio, A. Covello, and N. Itaco, Phys. Rev. C **65**, 051301(R) (2002).
[35] T. T. S. Kuo, S. Y. Lee, and K. F. Ratcliff, Nucl. Phys. **A176**, 62 (1971).
[36] K. Suzuki and S. Y. Lee, Prog. Theor. Phys. **64**, 2091 (1980).
[37] L. Coraggio, A. Covello, A. Gargano, N. Itaco, and T. T. S. Kuo, J. Phys. G **26**, 1697 (2000).
[38] A. Covello, F. Andreozzi, L. Coraggio, A. Gargano, and A. Porrino, in *Contemporary Nuclear Shell Models*, Lecture Notes in Physics Vol. 482 (Springer-Verlag, Berlin, 1997).
[39] F. Andreozzi, L. Coraggio, A. Covello, A. Gargano, T. T. S. Kuo, Z. B. Li, and A. Porrino, Phys. Rev. C **54**, 1636 (1996).